

Article

Adaptive Cruise Control in Electric Vehicles with Field-Oriented Control

Ana-Maria Petri * and Dorin Marius Petreus 

Applied Electronics Department, Faculty of Electronics, Telecommunications and Information Technology, Technical University of Cluj-Napoca, 400114 Cluj-Napoca, Romania; dorin.petreus@ael.utcluj.ro

* Correspondence: ana.petri@ael.utcluj.ro

Abstract: An adaptive cruise control system is highly used in conventional internal combustion engine vehicles, but due to the electrification of the vehicles, the adaptive cruise control system must be placed in relation with the electric motor control block. This paper presents the relationship between an adaptive cruise control system and the motor control in the case of an electric vehicle. An indirect field-oriented control of an induction machine is considered for the electric traction system. The adaptive cruise control block computes the required acceleration to ensure the velocity set by the driver based on the set velocity, the actual velocity of the vehicle, a safe distance, and the relative distance between the host car and a leading car. The proposed system was implemented in MATLAB/Simulink and, also, in a low-scale laboratory experimental setup. The correct operation of the system was tested using a speed profile, and both systems, simulated and experimental, have the expected response. The velocity, acceleration, rotor speed, torque response, and relative and safe distance are the responses presented to prove the efficiency of the proposed implementation.

Keywords: adaptive cruise control; electric vehicle; induction machine; field-oriented control; dSPACE



Citation: Petri, A.-M.; Petreus, D.M. Adaptive Cruise Control in Electric Vehicles with Field-Oriented Control. *Appl. Sci.* **2022**, *12*, 7094. <https://doi.org/10.3390/app12147094>

Academic Editor: Gang Lei

Received: 31 May 2022

Accepted: 12 July 2022

Published: 14 July 2022

Publisher's Note: MDPI stays neutral with regard to jurisdictional claims in published maps and institutional affiliations.



Copyright: © 2022 by the authors. Licensee MDPI, Basel, Switzerland. This article is an open access article distributed under the terms and conditions of the Creative Commons Attribution (CC BY) license (<https://creativecommons.org/licenses/by/4.0/>).

1. Introduction

The transportation sector has great importance nowadays; there are more than a billion vehicles in the whole world, and the number is increasing exponentially, with expectations that in 10 years there will be more than 2 billion vehicles in the world [1].

The mainly used vehicles are those powered by internal combustion engines (ICE). Even though the first electric vehicle (EV) was created in the 1830s, after the development of the batteries, electric vehicle growth stopped in the 1900s due to the development of ICE-powered vehicles. ICE vehicles had great success because fossil fuels had lower prices than batteries; this is still accurate nowadays too, with the series production of ICE vehicles, so the overall price of the ICE vehicles was reduced. Additionally, the batteries had a low capacity and power density at that time, compared with gasoline, and ICE vehicles could travel long distances [2].

Over the past decades, climate changes and pollution issues have been considered, and the transportation sector is a pollution source because of the greenhouse gas emissions generated by the internal combustion engines. Given these issues, and also adding the limited resources of fossil fuels, the vehicle industry is searching for an alternative solution for transportation. Electric vehicles are a perfect alternative for transportation, without greenhouse gas emissions and without fossil fuel consumption. So, in the last years electric vehicles have gained more interest because they are a suitable replacement for the classic vehicle with an internal combustion motor. Electric vehicle growth is also based on the development of batteries. Lithium batteries have a higher power density and capacity than other batteries and made possible the use of electric vehicles, but there is still a problem about the range and time required for the battery to be charged [2–4].

The major advantages of electric vehicles over ICE vehicles are the reduced emissions of carbon monoxide emissions and that there is the higher efficiency and performance

of the electric motor than the ICE engine because the electric traction system has fewer mechanical parts and gears, which reduces a huge number of mechanical losses and, also, lowers maintenance costs [3].

An efficient driving style or eco-friendly driving style is an important aspect considered for ICE vehicles to reduce fuel consumption, and it is even more important for EVs because it can extend the driving range. Driving style is particular to each driver, but there have been some driving assistant systems developed that help drivers have a better driving experience. One of the popular driving assistant systems is cruise control (CC), which maintains a constant vehicle speed, improves fuel economy, and increases driver comfort during long-distance driving [5–11].

Cruise control is a driving assistance system that allows the driver to set a desired speed, and the system ensures that the vehicle has a set speed so the driver does not have to keep the acceleration pedal pushed to maintain a certain speed; this is the basic cruise control application [6,8,10].

The first cruise control system was developed in 1950 by the engineer Ralph Teetor, who patented a “Speed Control Device for Resisting Operation of the Accelerator” [12].

The first generation of cruise control systems had only mechanical parts used to keep the throttle in a fixed position to maintain a constant speed. In the following years, the system was improved with electronic components, such as speed sensors, a microcontroller for control, and providing a user interface; therefore, the throttle actuator was easier to control in various positions for different values of speed [10].

An updated version of the cruise control system is the adaptive cruise control (ACC) system; cruise control controls the speed of the vehicle, but adaptive cruise control controls the speed but also the distance between the host vehicle and a leading vehicle [8].

Advanced cruise control systems focus on accelerating or braking so that the vehicle speed is constant at the set value but, also, a safety driving distance is ensured. The internal combustion motor is accelerated if needed, through the throttle actuator, and braking is performed using a braking system [10,11,13].

For electric vehicles, the implementation of cruise control is a little different because the electric motor can accelerate or brake, in a defined range, based on the value of the current supplied through the inverter. The electric motor control can generate driving signals to accelerate, brake, or, even, to work as a generator in regenerative braking mode. Therefore, in electric vehicles, the cruise control system should relate to the motor control system for high efficiency [10,11,13–17].

To analyze the speed of a vehicle is important to know how the motor works and how its speed is controlled. In the case of an electric vehicle, there is an electric motor. Electric motors have a great advantage over internal combustion motors, the ability to work as a generator, so that regenerative braking is possible in electric vehicles. For a propulsion system, there are some specific requirements that the electric motor must have, such as high power and torque density, wide speed range, high torque for start and hill climbing, and a wide range for constant power. Based on these requirements, the following electric machines can be used in electric vehicles: DC machines, induction machines, switched reluctance machines, brushless DC machines, and permanent magnet synchronous machines. BLDC and permanent magnet synchronous machines proved to have a higher efficiency but with a higher cost, and with the possibility of the demagnetization of the permanent magnets [18–21].

For an electric propulsion system, it is important to control the torque and speed of the electric machine so that the vehicle can overcome the starting torque and to deliver the desired speed. The control of an induction machine can be performed in many ways, but for higher efficiency, two control strategies are widely used: field-oriented control (FOC) and direct torque control (DTC) [20]. Field oriented control ensures the proper control of an induction machine, using a d-q representation to control variables as dc quantities using basic PI controllers [22,23]. Field oriented control can be implemented sensorless, many

papers have presented different methods [24–27]. Additionally, field-weakening control can be applied along with field-oriented control to achieve a higher speed [28,29].

Nowadays, the development of electric vehicles determines the implementation of new driving assistance systems or the adaptation of the older ones so that they can be successfully used also in electric vehicles. Being a useful system, cruise control adaptation for electric vehicles is required.

This study presents how an adaptive cruise control system interacts in an electric vehicle with an induction machine controlled with an indirect field-oriented method. In the literature, the two systems are presented and discussed, but the relation between them and how the two systems are connected is not mentioned anywhere. That is the goal and novelty of this paper, to illustrate the function of an adaptive cruise control system in an electric vehicle powered by an induction machine controlled with an indirect vector control in the case of the cruise control scenario. This paper presents only the electric part of the powertrain system of an electric vehicle; no mechanical components as a brake, distribution, or wheels were considered for this study.

The contributions of this paper are the following:

- Illustrates how adaptive cruise control works for an electric vehicle having an induction motor controlled in an indirect field-oriented manner.
- Presents the relationship between an adaptive cruise control system and field-oriented induction machine control system in the case of an electric traction system.
- Tests the efficiency of an electric powertrain system with an induction machine when adaptive cruise control is considered.
- Using a dSPACE platform, a low-scale laboratory prototype system was implemented, allowing the development of a digital field-oriented control.
- The simulation results and experimental ones prove the efficiency of the proposed and implemented system for an electric propulsion system.

The next section introduces the theoretical aspects of adaptive cruise control. Then, the principals of field-oriented control are presented in Section 3. The system implementation is illustrated in Section 4 and the results in Section 5. The results are discussed in Section 6, and the last section concludes the findings of this paper.

2. Adaptive Cruise Control

Cruise control allows driving at a constant set speed value without the need to keep the acceleration pedal pushed. This provides more comfort for the driver and ensures safe operation. The classic variant of cruise control endures only speed control, and an updated version is adaptive cruise control [6,8,10].

In the last decades advanced variants of cruise control were implemented based on the front radar. Advanced Driver Assistance Systems, known as ADAS in the literature, provide various technologies for driving assistance. One of the main technologies in the ADAS group is an adaptive cruise control system, having the ability to accelerate so that the vehicle speed is kept as the set value, but using a distance sensor, it is possible to detect if there is another vehicle in front, so a lower constant speed is set to ensure a safe distance between the vehicles [8,11].

Advances in radar application and intelligent control systems have allowed the development of several other variants of cruise control. For classic vehicles, a cruise control system can ensure economical driving, but that is not really the purpose; it is more a driving safety and comfort option. Electric vehicles, on the other hand, still must handle the range anxiety problem, and some studies have shown that efficient driving can still extend the vehicle range. Therefore, many advanced cruise control variants were developed, such as efficient cruise control, predictive cruise control, optimized cruise control, and other variants in which, besides safe driving distance, the traffic signal status is also considered to predict braking [5–9].

Adaptive cruise control has two control loops: one is the classic speed control, such as in cruise control; the control block keeps the vehicle running at the set speed value. The

second control loop is a distance control, which involves scanning the road and in case there is another vehicle ahead, the set speed is adjusted to keep a safe distance between the host vehicle and the detected leading vehicle. To detect leading vehicles and obstacles on the road, adaptive cruise control requires radar or laser sensors to scan the road [8,11,13,30,31].

When there is no vehicle or obstacle in front of the host vehicle, adaptive cruise control works only in the speed mode, while in classic cruise control, the vehicle is running with the driver's set speed value [11,13,30,31].

When a leading car is detected, the inter-vehicle distance is determined and compared with the safe distance value. If the inter-vehicle distance is higher than the safe distance value that the host vehicle is running at the set speed value, the adaptive cruise control system works in the speed mode. If the intervehicle distance is lower than the safe distance value, than the host vehicle speed is adjusted to ensure a safe distance between the vehicles, so the adaptive cruise control works in the safe distance mode [8,11,13,30,31]. Figure 1 illustrates the two modes of operation of an ACC system.

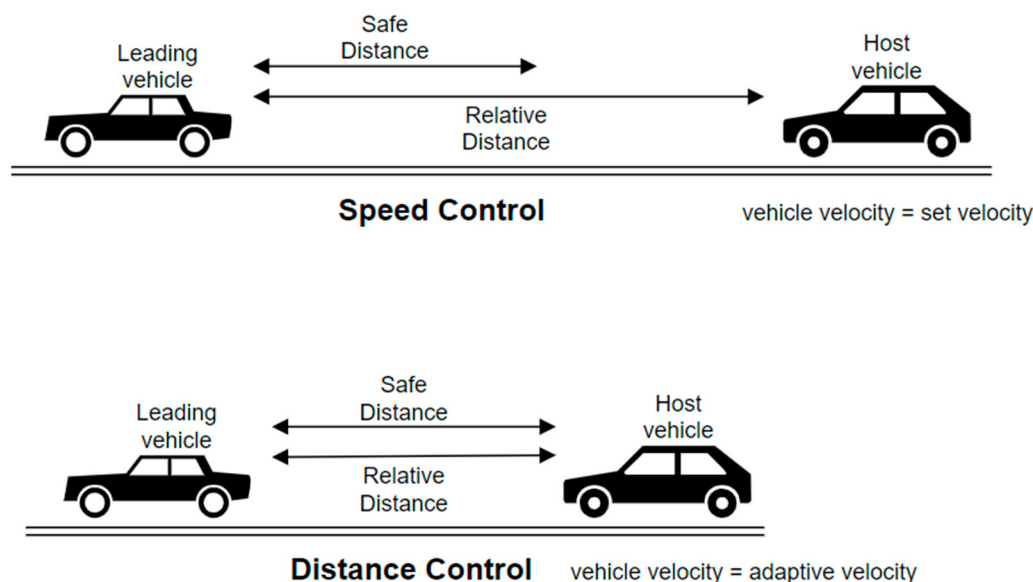


Figure 1. Working modes of adaptive cruise control.

The inter-vehicle relative distance is determined based on the initial distance between the two vehicles (d_0), the velocity of the host car (v_{host}), and a time constant (t_{safe}) that ensures a safe time for the driver safe brake reaction. The inter-vehicle safe distance is obtained using Equation (1), as follows:

$$d_{safe} = d_0 + t_{safe} \cdot v_{host} \quad (1)$$

Regardless of the operating mode, the ACC system should provide the corresponding acceleration to ensure the desired velocity or the safe distance. For ICE vehicles, the commands from ACC are applied to the throttle control block. Based on the acceleration value from the ACC block and the throttle position sensor, the throttle valve is controlled based on the acceleration from the ACC block and the feedback from the throttle position sensor. Figure 2 presents a block diagram of an ACC system in the case of an ICE vehicle.

In an EV, there is no throttle valve, throttle control, or throttle position sensor; the engine is replaced with an electric machine, and the acceleration of the motor is handled by the motor control block through the inverter. Therefore, for an EV, the ACC block output signal is applied to the motor control block—in this paper, an indirect field-oriented control block.

In the same manner as in the ICE vehicle, the field-oriented control block is based on the acceleration ratio set by the ACC block, and the motor speed feedback signal generates the corresponding PWM driving signals for the inverter to control the electric machine

working mode (motor or generator) and required speed. Figure 3 illustrates a block diagram of an EV with an ACC system.

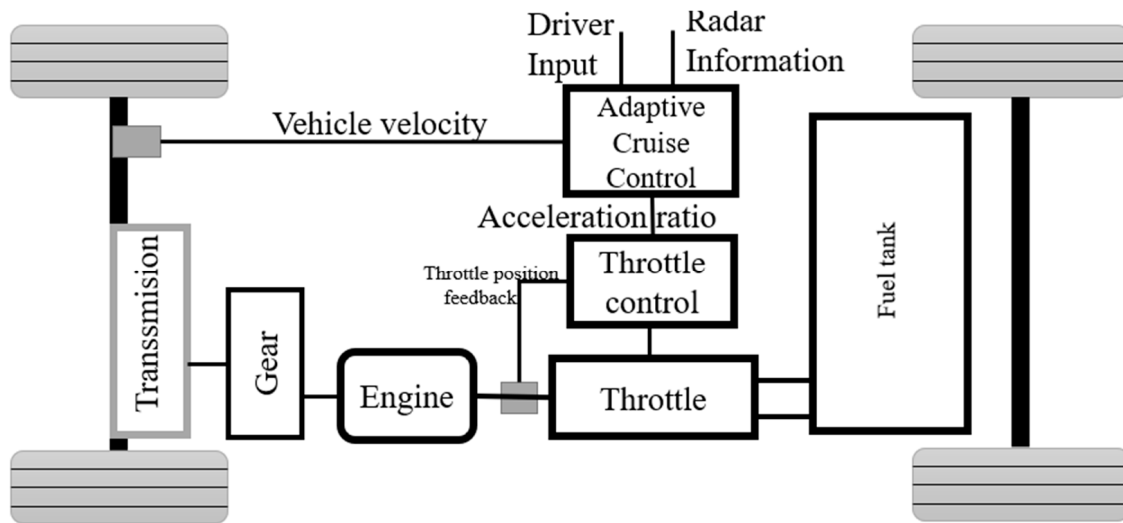


Figure 2. ICE propulsion system with adaptive cruise control.

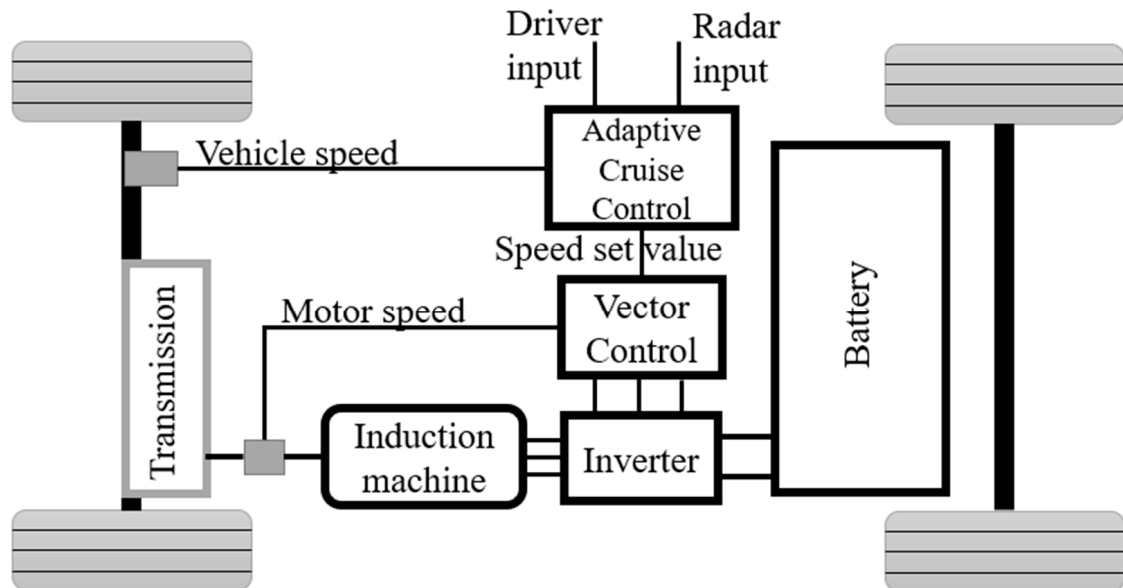


Figure 3. EV propulsion system with adaptive cruise control.

In comparison with the ICE vehicle, the EV has fewer mechanical and moving parts, and the motor control block through the inverter handles the acceleration without throttle, throttle control, or a throttle position sensor so there are fewer maintenance costs and, also, fewer mechanical losses; therefore, the efficiency of the vehicle increases.

The overall efficiency of EVs is higher also because electric machines have a higher efficiency compared with the ICEs used in classic vehicles. Vehicle torque should be high at low speeds and decrease as the speed increases. One should note that, because ICE does not have, by nature, the corresponding torque-speed characteristics, ICE vehicles have a gear box. Meanwhile, the torque-speed characteristics of the electric machine are exactly what is needed for vehicles. The torque-speed characteristics of the electric machine and ICE are presented in Figure 4.

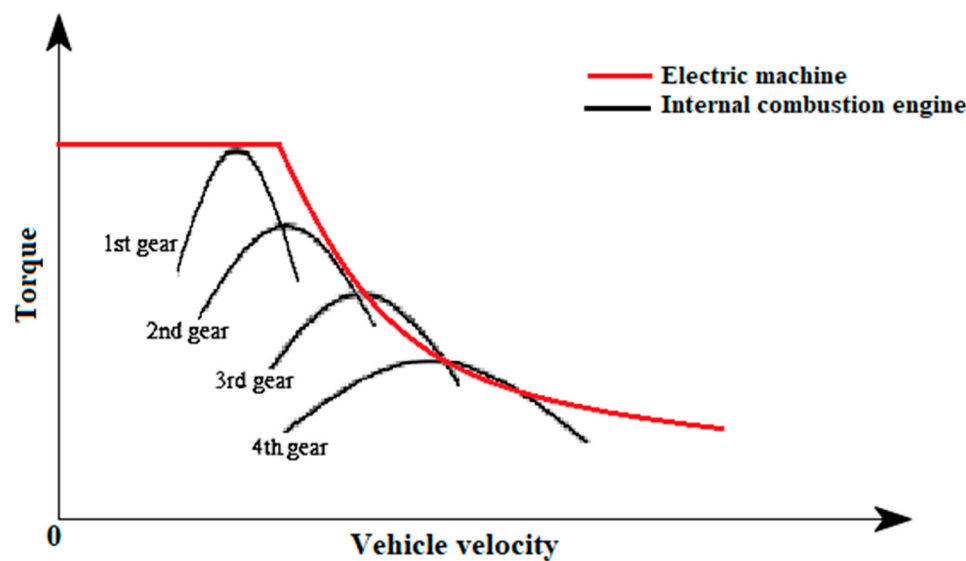


Figure 4. Torque-speed characteristics of electric machine and internal combustion engine.

Regardless of the vehicle type, there are many adaptive cruise control methods developed and that are currently under development. The focus of this paper is not the implementation of adaptive cruise control but to present how the output of the ACC block is applied to an indirect field-oriented control block. To prove the concept of an ACC in an electric vehicle, a simple ACC block was used in this paper.

The ACC block used in this paper requires a set velocity value as the velocity set by the driver, a time gap value, a feedback value of the longitudinal velocity of the ego vehicle, the longitudinal velocity of the leading vehicle, and the relative distance between the two vehicles. A default safe distance is set to 10 m. The variables enumerated previously are applied to a Model Predictive Control (MPC). The output of the ACC block is the output of the MPC and represents the longitudinal acceleration/deceleration, which is applied to the input of the field-oriented control block.

The ACC output can be a positive or a negative value. When the output is a positive value, it represents an acceleration, which is transformed in angular velocity and added to the speed reference of the field-oriented control. In the opposite case, when the output value of the ACC is a negative value, it means that the vehicle should decelerate, and adding a negative value to the speed reference of the field-oriented block will result in a smaller value of the reference speed, so the vehicle speed will decrease; this is as the engine brake in the case of the ICE vehicle. A real vehicle also has a mechanical brake for a full stop, but in this paper, the mechanical parts of the vehicle are not considered; only the deceleration base on the engine brake is presented.

The MPC has the following inputs: measured outputs of the system, an output reference value, and a disturbance signal that affects the system. In the ACC case, the measured variables are the longitudinal velocity of the ego vehicle and the relative distance between the vehicles. For the reference value, the set velocity and the default safe distance are required. The disturbance is the velocity of the leading vehicle. Based on these inputs, the ACC with MPC has the following algorithm:

1. The safe distance is calculated using Equation (1).
2. An adaptive velocity reference is calculated as follows:

$$v_{ACCref} = v_{lead} - K_p(d_o - d_{relative}) \quad (2)$$

3. The adaptive velocity reference is compared with the set velocity: if the adaptive speed is larger than the set velocity, then velocity reference is the velocity value set by the user, and the vehicle is accelerated to reach the corresponding velocity in speed control mode. Otherwise, if the adaptive speed is lower than or equal to

In two different modes

the set velocity, then the reference value is the adaptive velocity, and the vehicle is accelerated or decelerated to maintain the safe distance between the vehicles in distance control mode.

4. Based on all these variables, the MPC calculates the corresponding acceleration/deceleration value.

In Figure 5 is presented a block diagram of the ACC system.

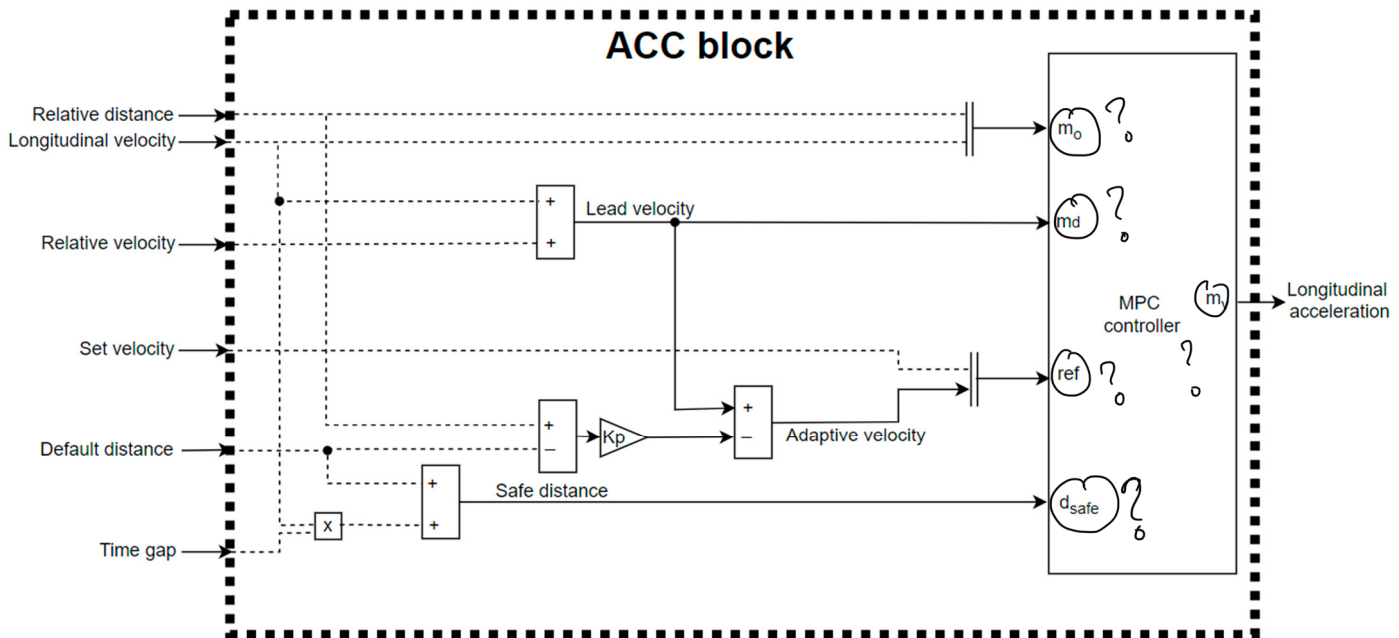


Figure 5. Adaptive cruise control block diagram.

3. Field-Oriented Control

In field-oriented control, the induction machine is seen as a separated excited DC machine. In a DC machine, the field current is perpendicular to the armature current, so there are no coupling effects. The analogy with the separate excited DC machine is made using a d-q synchronous equivalent circuit, where the three-phase stator currents (i_a , i_b , and i_c) are transformed in two orthogonal currents (i_{ds} and i_{qs}). While in a separately excited DC machine for a proper control, it is enough to control each current, for the induction machine using vector control i_d and i_q as the control variables, i_d current is aligned with the field, and i_q is in the same direction as torque. In this way, field-oriented control allows the independent control of the two currents and a higher efficiency is achieved [2,8,23–26].

An important part of vector control development is determining the synchronous rotating angle (θ_e) of the d-q synchronous rotating representation. The correct determination of the synchronous rotating angle determines the correct alignment of i_{ds} with the flux and i_{qs} perpendicular to it. Based on how the synchronous rotating angle is determined, there are two methods for implementing vector control: direct vector control (feedback method) and indirect vector control (feedforward method). In this paper, only indirect vector control method will be analyzed [8].

Indirect vector control uses the slip frequency expression. As is known, the slip frequency equals the difference between the synchronous frequency and rotor frequency. Using the slip expression, the synchronous rotating angle is determined as follows:

$$\theta_e = \int \omega_e dt = \int (\omega_r + \omega_{sl}) dt = \theta_r + \theta_{sl} \quad (3)$$

For a squirrel cage induction machine, the rotor windings are short-circuited and $v_{dr} = v_{qr} = 0$; thus, the expressions of the rotor voltages can be written:

$$v_{qr} = \frac{d}{dt} \Psi_{qr} + R_r i_{qr} + (\omega_e - \omega_r) \Psi_{dr} = 0 \quad (4)$$

$$v_{dr} = \frac{d}{dt} \Psi_{dr} + R_r i_{dr} - (\omega_e - \omega_r) \Psi_{qr} = 0 \quad (5)$$

Using the stator currents, the rotor flux linkages, magnetizing, and rotor inductions, even though the rotor currents cannot be measured, their expressions are:

$$i_{qr} = \frac{1}{L_r} \Psi_{qr} - \frac{L_m}{L_r} i_{qs} \quad (6)$$

$$i_{dr} = \frac{1}{L_r} \Psi_{dr} - \frac{L_m}{L_r} i_{ds} \quad (7)$$

The rotor currents in (4) and (5) can be eliminated by the expressions from (6) and (7); thus, the following equations are obtained:

$$\frac{d}{dt} \Psi_{qr} + \frac{R_r}{L_r} \Psi_{qr} - \frac{L_m}{L_r} R_r i_{qs} + \omega_{sl} \Psi_{dr} = 0 \quad (8)$$

$$\frac{d}{dt} \Psi_{dr} + \frac{R_r}{L_r} \Psi_{dr} - \frac{L_m}{L_r} R_r i_{ds} + \omega_{sl} \Psi_{qr} = 0 \quad (9)$$

To assure the decoupling between flux and torque, the rotor flux Ψ_r will be only on the d axis, so the q component of the rotor flux will be zero:

$$\Psi_{qr} = 0 \quad (10)$$

If Ψ_{qr} is zero, then its derivative is also zero:

$$\frac{d}{dt} \Psi_{qr} = 0 \quad (11)$$

Using the information from (10) and (11) in Equation (8), the expression of the slip frequency is the following:

$$\omega_{sl} = \frac{L_m R_r}{\Psi_r L_r} i_{qs} \quad (12)$$

Additionally, the rotor flux is aligned with i_{ds} current and has the following expression:

$$\Psi_r = L_m i_{ds} \quad (13)$$

All the assumptions made also affected the torque expression, and it can be characterized by the following equation:

$$T_e = \frac{3}{2} \left(\frac{P}{2} \right) \frac{L_m}{L_r} \Psi_r i_{qs} \quad (14)$$

When working with electric machines, as in this case with an induction machine, it is important to also know the mechanical behavior of the machine. The rotor speed depends on the mechanical speed (ω_m) and the number of poles in the machine. The mechanical speed is the actual speed of the machine and is influenced by the load torque (T_L) and rotor inertia (J) based on the following equation:

$$T_e = T_L + J \frac{d\omega_m}{dt} = T_L + \frac{2}{P} J \frac{d\omega_r}{dt} \quad (15)$$

To develop a vector control loop for an induction machine, Equations (12)–(14) and the stator current and mechanical speed measurements are required. Figure 6 presents a block diagram of an induction machine drive system with field-oriented control, where the i_{qs} current is controlled in a closed loop. The set value of i_{qs} is obtained based on Equation (14), where the torque is determined from the speed error, and for the flux, Equation (13) is used and the i_{ds} current, all this using the speed and stator current feedback. i_{ds} current is controlled in an open loop, using the rated current of the motor, to obtain a maximum flux.

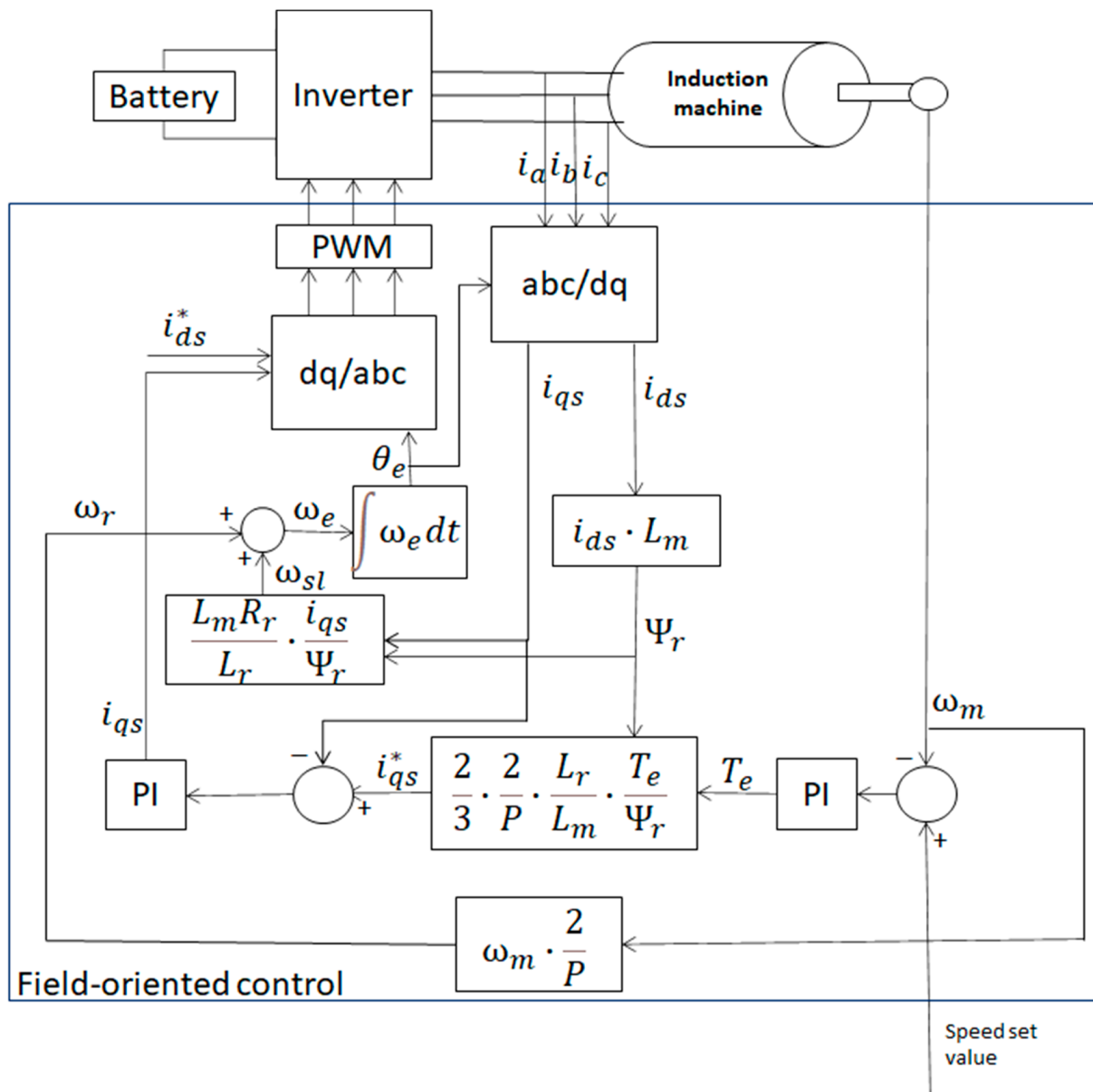


Figure 6. Vector-controlled induction machine system. Reproduced from [18] with permission from IEEE.

The paper's goal is to illustrate the relation between motor control and cruise control; therefore, Figure 7 presents the control block of an electric vehicle considering the cruise control system, vector control system, torque load disturbance, sensors, and vehicle transmission system.

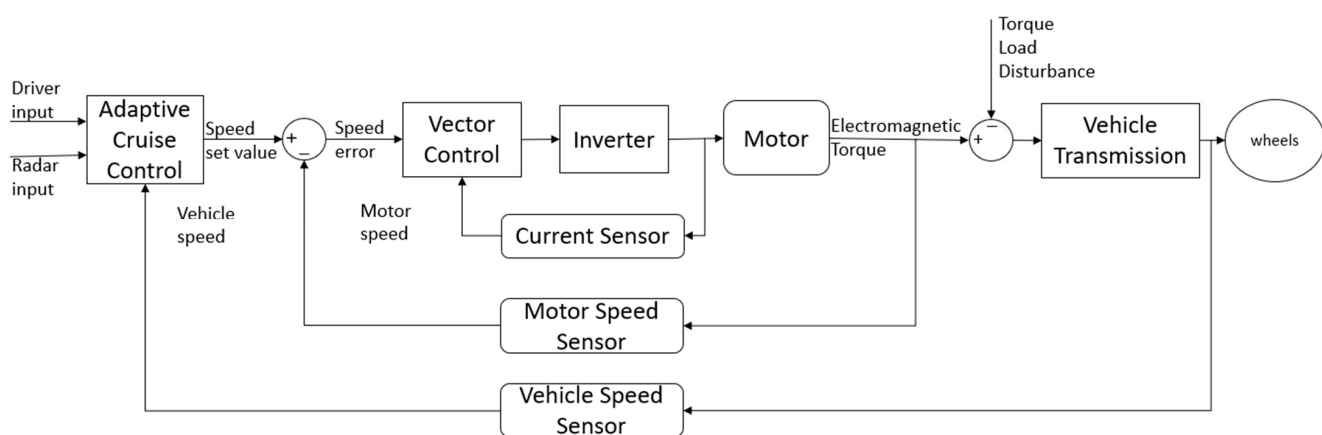


Figure 7. EV control system with adaptive cruise control.

4. Implementation

This section illustrates the implementation of a low-scale laboratory powertrain system and presents the relationship between the cruise control and vector control of the induction machine. Starting from the block diagram, in Figure 4, in the first stage, a simulation was developed to test the validity of the system. After the simulation was implemented and the efficiency of the control loop was proved, an experimental system was developed using a Lesson 1/3 HP 3450 rpm induction machine with the following characteristics presented in Table 1.

Table 1. Lesson induction machine parameters.

Parameter	Value
Rated Power	0.25 kW
Rated Voltage	230 V
Rated Current	1.4 A
Rated Frequency	60 Hz
Rated Speed	3450 rpm
Number of Poles	2
Stator Resistance (R_s)	8.4 Ω
Stator Leakage Inductance (L_{ls})	6.6 mH
Rotor Resistance (R_r)	2.35 Ω
Rotor Leakage Inductance (L_{lr})	6.8 mH
Magnetizing Inductance (L_m)	206 mH
Moment of Inertia (J)	0.00173 kgm ²
Friction Coefficient	0.0027 Nm/rad/s

To test the efficiency of the control loop in the presence of a torque load, a powder brake was used, so a specific torque was imposed on the motor. A B53 electromagnetic powder brake, from the Efex series, was used for this implementation.

This brake has three main elements: a coil, a stator, and a rotor. The brake was supplied with current so the coil started generating a magnetic field that varied proportionally to the intensity of the current. The variation in the magnetic field modified the viscosity of the powder situated between the stator and the rotor. In this way, the brake had an output torque proportional to the intensity of the supplied current. Figure 8 presents the current-torque characteristics of the brake.

To ensure stability and robustness in the control of the torque load, a current regulator was used to supply the electromagnetic brake. Leo is a microprocessor controlled digital current regulator that has a closed loop PWM current regulation to keep the specified torque stable. Leo was designed accordingly to the B53 powder brake, and it has an output current variation between 0 and 1 amperes, which is proportional to the input voltage. The input voltage can be generated by a potentiometer for a manual interaction with the system.

or it can be set using a PLC or other devices with a voltage output, with a range between 0 and 10 Vdc.

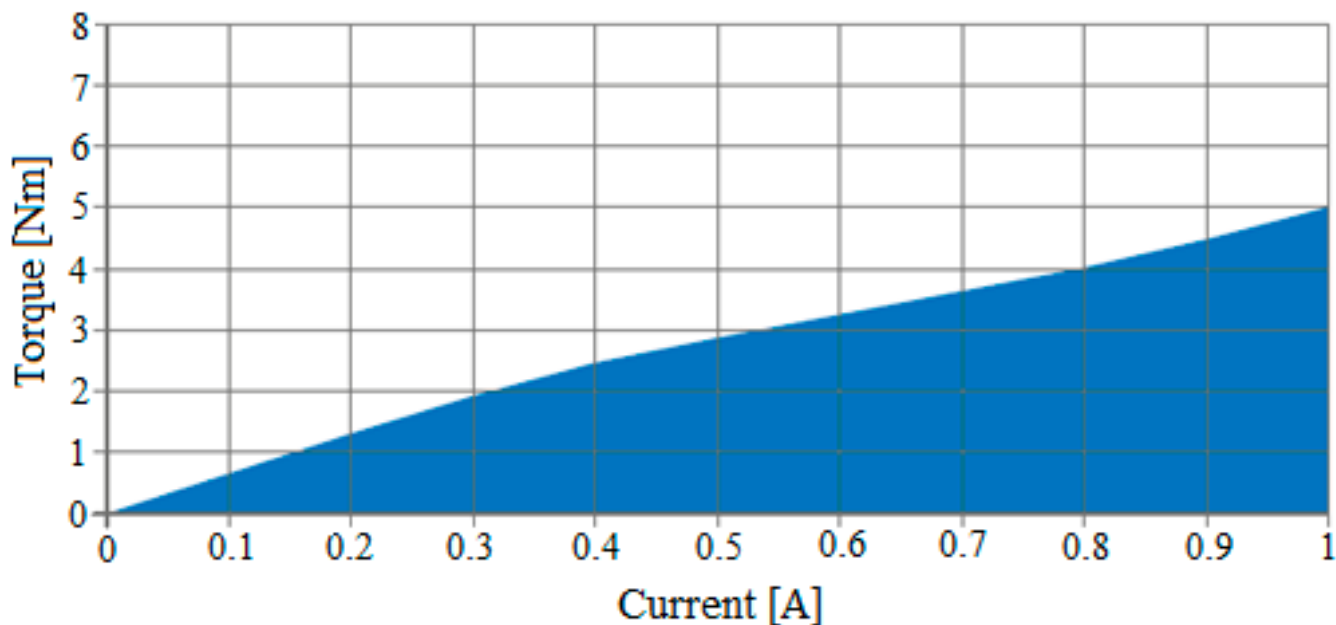


Figure 8. Current-torque characteristic of the powder brake.

• Simulation

The simulation of the adaptive cruise control based on an indirect field-oriented control drive system was implemented in the Simulink environment from MATLAB. To simulate the same system as the experimental one, the simulated elements had the same parameters as the real elements used in the low-scale prototype system. The induction machine was modeled based on the parameters from Table 1 to obtain an accurate view of how the experimental setup will work. Then, the motor was supplied through an IGBT inverter from a DC source, which acts like a battery. The inverter was driven by PWM signals, which were generated with an SPWM generator based on the sinusoidal three-phase current generated from d-q currents obtained from the vector control block. Additionally, the electromagnetic brake and current regulator were modeled and simulated.

The adaptive cruise control block respects the structure presented in Figure 4, and it generated longitudinal acceleration based on the set driving speed, the safe time gap in seconds, the relative distance between the vehicles, the relative velocity between the vehicles, and the host vehicle speed, as presented in Section 2. Besides the host vehicle system, a leading vehicle was also modeled. Figure 9 presents the simulated system.

This simulation allowed us to test three possible scenarios. The first one was when there was no car in front of the host car; the host car can run at the desired set velocity in this classic cruise control scenario. The second scenario was when the host car was running at the desired set velocity and at a certain point in time, and there was a leading car in front, so the velocity must be adjusted to maintain a safe distance between the two vehicles. The third scenario was when the host car was following a leading car for a certain period, so the velocity was adjusted to maintain a safe distance.

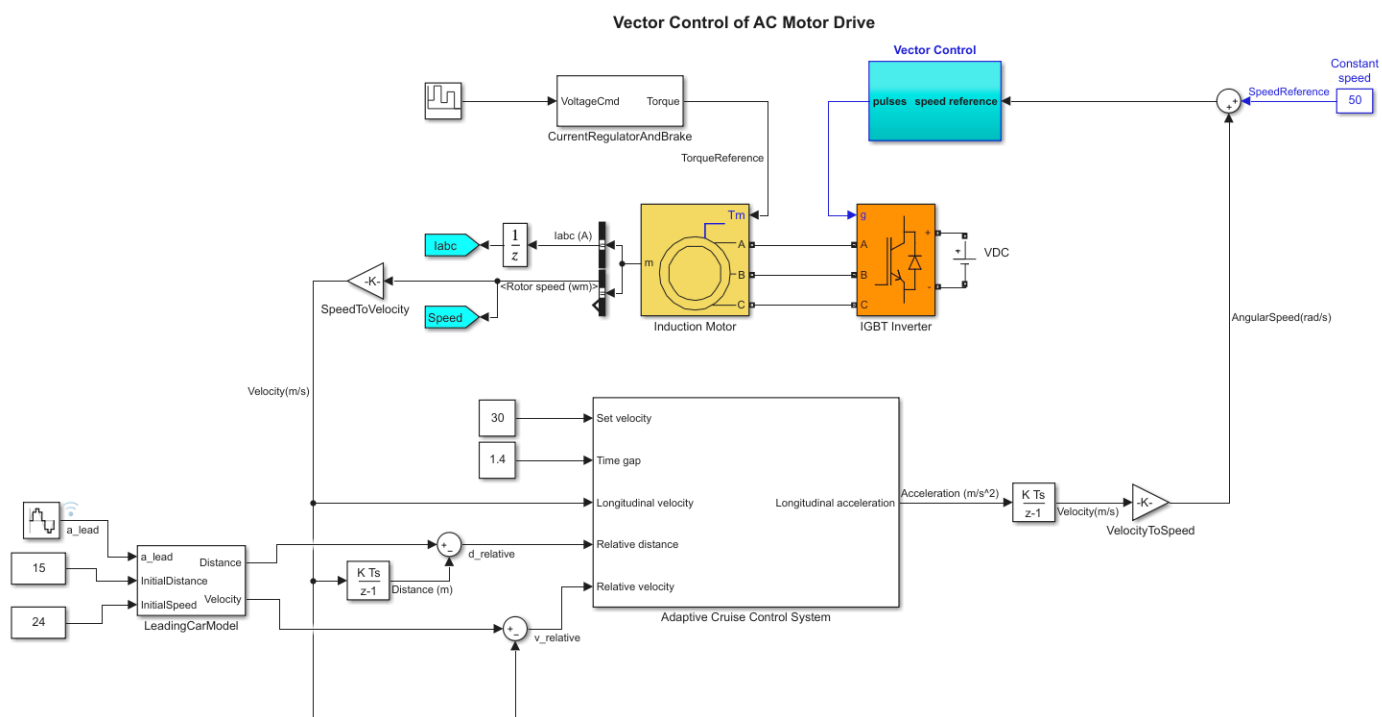


Figure 9. Adaptive cruise control based on indirect vector-controlled induction machine drive system.

The vector control block was the implementation of an indirect vector control based on Equations (12)–(14), the block diagram from Figure 4, and the machine's parameters from Table 1. Figure 10 presents the implementation of the indirect vector control block.

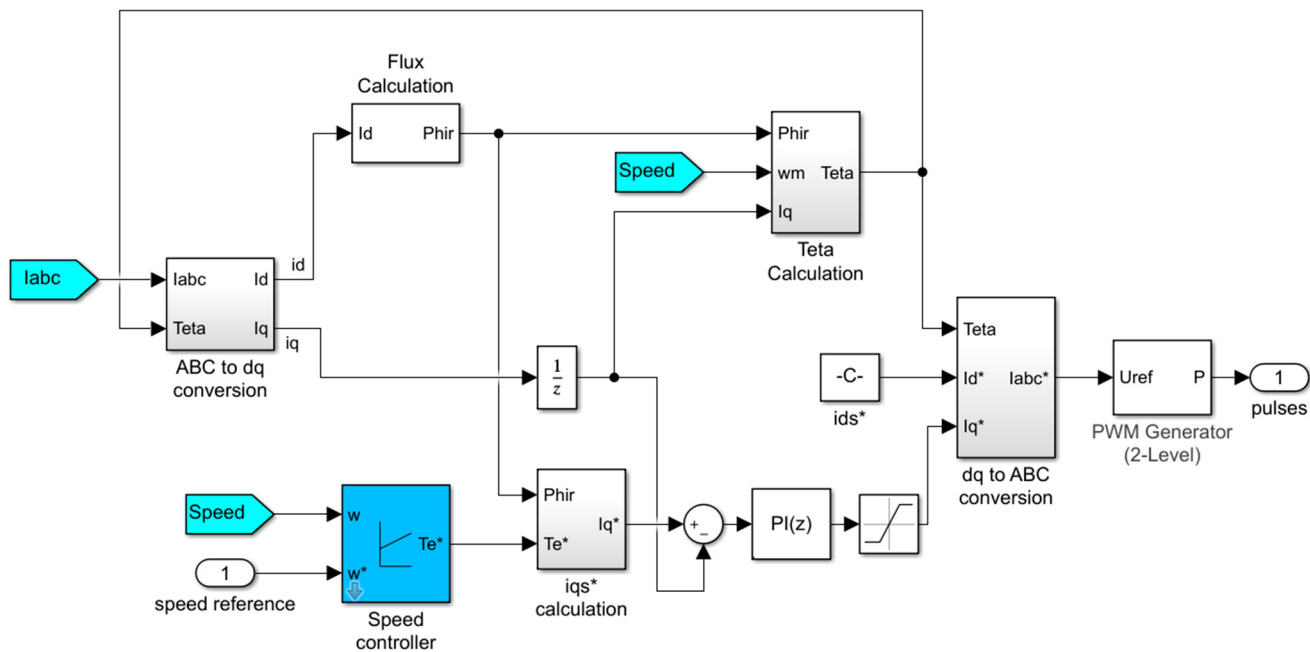


Figure 10. Indirect vector control block. Reproduced from [18] with permission from IEEE.

As in the case of the motor, the current regulator and the powder brake were also modeled based on the real element. The current regulator was modeled as a PWM signal generator, where the input voltage ranging between 0 and 10 V determined the duty cycle of the PWM signal from 0% to 100%. The PWM generated by the current regulator was applied to the brake, where using a transfer function, the PWM signal was transformed

into the current. Based on the current-torque characteristic, from Figure 4, a look-up table was implemented, so the corresponding torque was obtained at the output of the brake and was applied to the induction machine. Figure 11 illustrates how the brake was modeled.

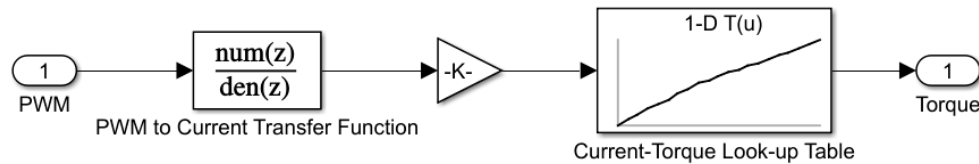


Figure 11. Electromagnetic powder brake model in Simulink.

- **Experimental system**

For the experimental system, beside the induction machine, Lesson 1/3 HP 3450 rpm, the current regulator, and electromagnetic powder brake, presented earlier, the following elements were used: a Danfoss inverter, a rotary encoder, three Hall current sensors, a power supply source, and a dSPACE platform.

The dSPACE platform has analog and digital inputs and outputs; it is a real-time, dual-core processor that can be programmed using Simulink. For this system, the dSPACE platform was used to read the signals from the current sensors and from the rotary encoder using Simulink; the vector control block was developed, and PWM drive signals for the inverter were generated.

Additionally, the torque load from the powder brake was controlled from the dSPACE using a voltage signal to the LEO—current regulator. Figure 12 presents the block diagram of the experimental system used to test the indirect vector control of an induction machine, and in Figures 13 and 14, there is a test bench experimental system.

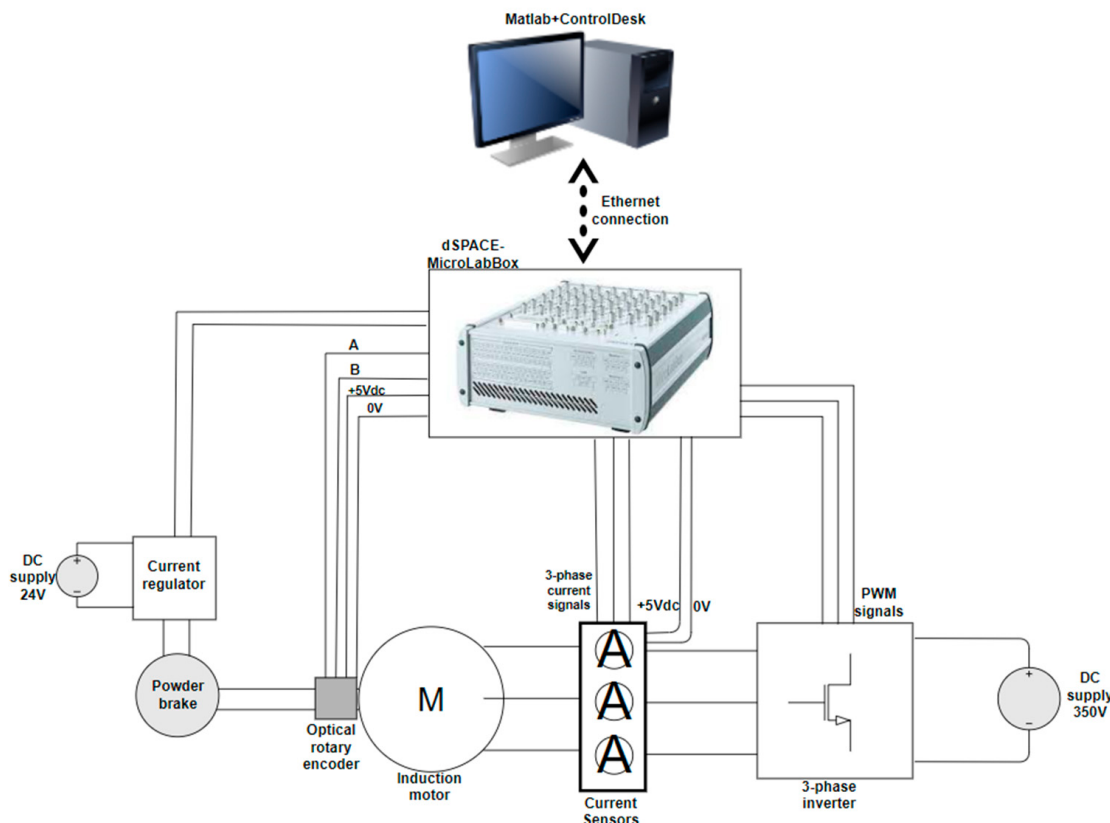


Figure 12. Block diagram of the experimental adaptive cruise control using an indirect vector control induction machine drive system.

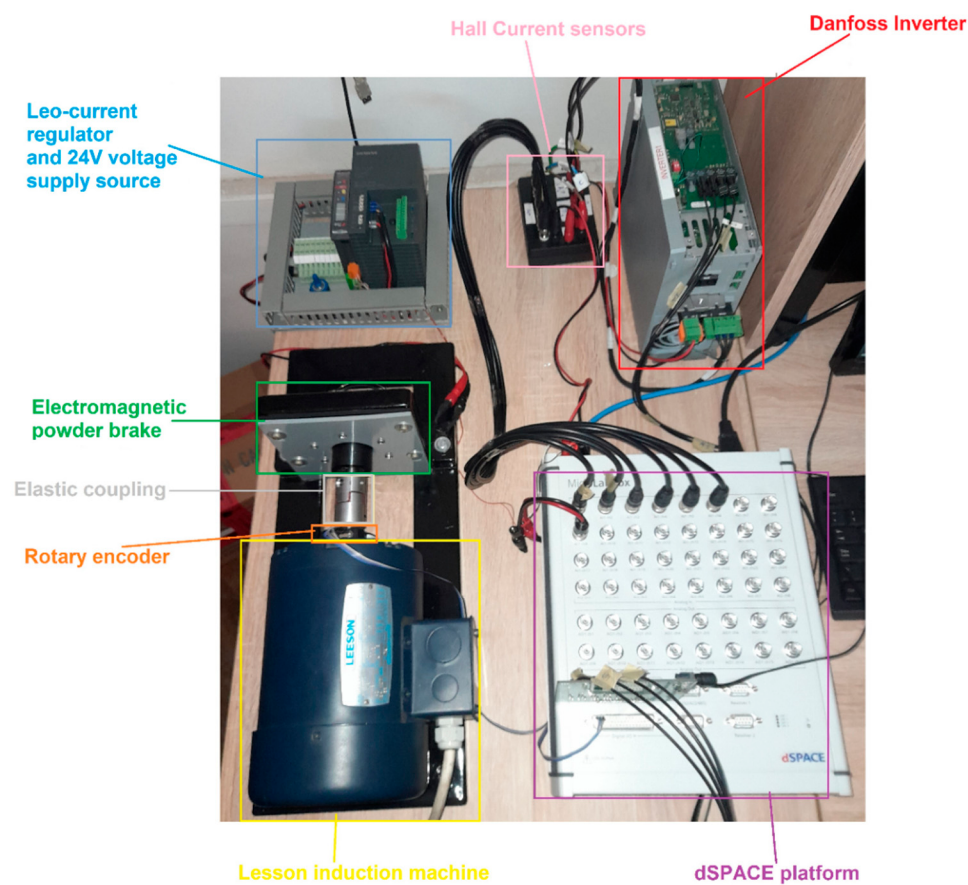


Figure 13. Low-scale laboratory experimental setup.

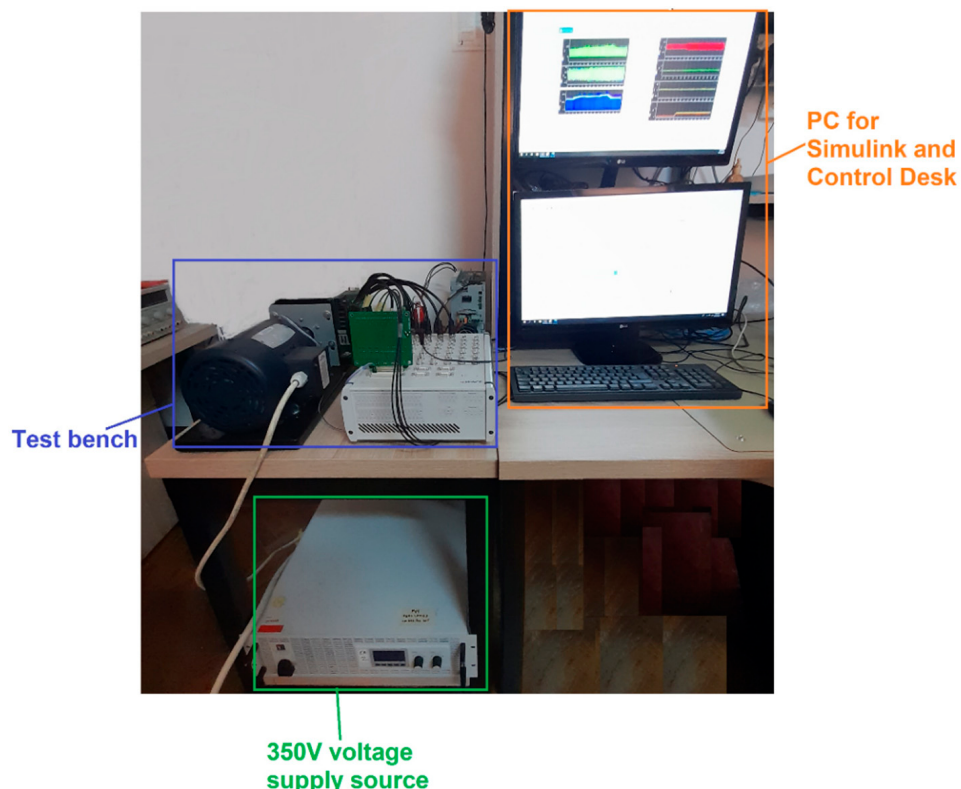


Figure 14. Experimental system.

The control block was developed in Simulink in the same manner as the block from the simulation; a difference in the experimental implementation was the use of real-time blocks needed to read the inputs from the sensors and to set the outputs for the driving signals. Another difference was that in the experimental development, there were required filters to eliminate the noise from the inputs. Additionally, the machine torque was estimated using Equation (14) and the i_{qs} current. Figure 15 presents the Simulink implementation of the control block used to program the dSPACE platform.

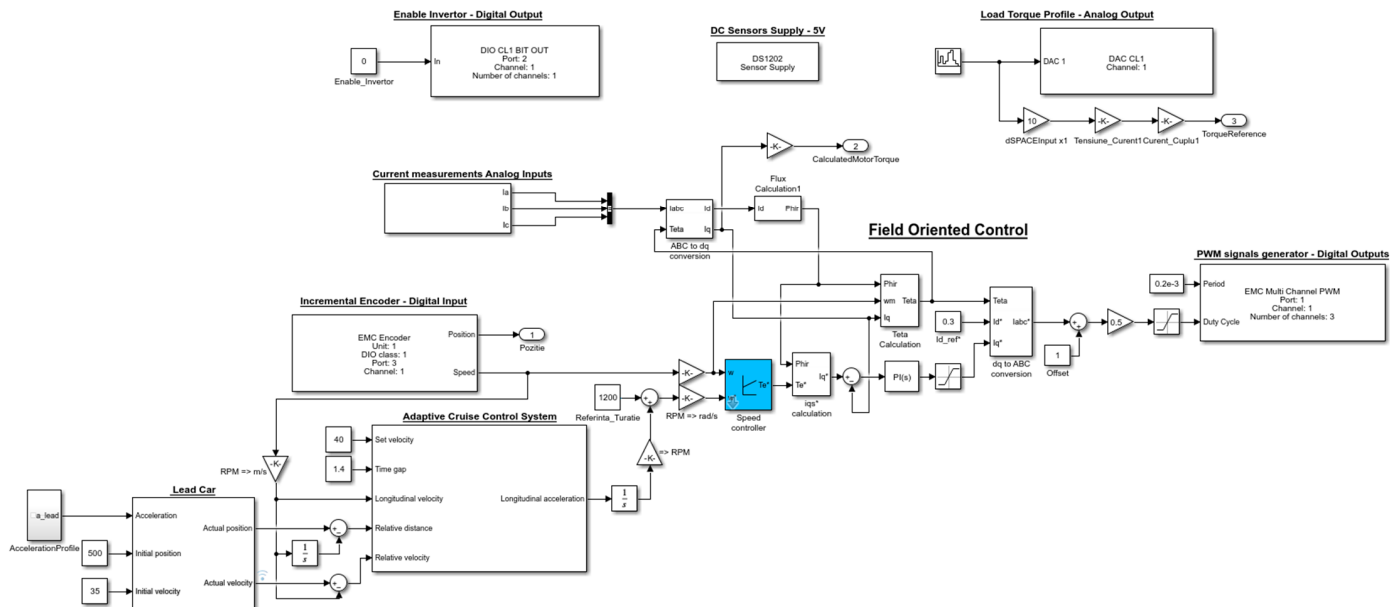


Figure 15. Simulink implementation of the control block used to program dSPACE platform.

The following section there presents the results obtained in the simulation and from the experimental system to prove the efficiency of the system in the adaptive cruise control scenario.

5. Results

The simulation and the experimental test bench were used to test the proposed system in an adaptive cruise control scenario. For the tested scenario, the velocity of the host vehicle was set at 40 m/s, so the adaptive cruise control system must ensure the corresponding acceleration. If there was no leading vehicle, the host vehicle ran at 40 m/s regardless of the torque load.

A speed profile was created for the leading car. It should be noted that the same speed profile was used in both the simulation and experimental setup. However, in the simulation, the scenario was performed quicker, and in fewer seconds, to reduce the simulation time.

In the first part of the scenario, the leading vehicle had 35 m/s velocity; then the velocity increased to 42 m/s, again lowered to 36 m/s, and in the end, the velocity increased to 45 m/s. The host vehicle was set to run at a constant 40 m/s velocity. Eventually, every time the leading vehicle was running a lower velocity than 40 m/s, the host vehicle reached the leading vehicle, and the adaptive cruise control system switched from speed control to distance control to ensure a safe distance between the two vehicles.

The relative distance, which is the distance between the two vehicles, was constantly compared with the safe value; if a negative slope was observed in the relative distance value, then the acceleration value was lowered and the host vehicle velocity reduced to maintain a relative distance larger or at least equal to the safe distance; the safe distance was calculated using Equation (1).

The results for the described scenarios are presented in Figures 16–20; the simulated results are illustrated, and from Figures 21–25, the results were obtained from the experimental setup.

- **Results from simulation**

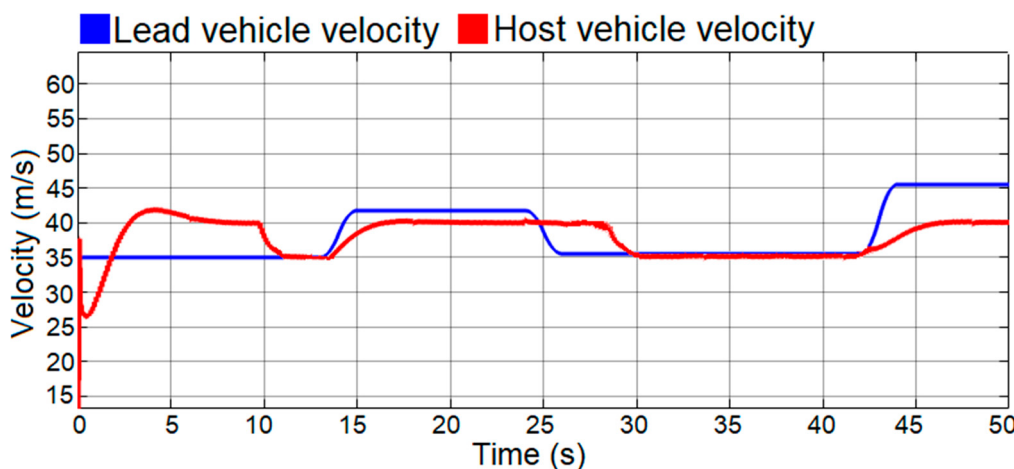


Figure 16. Velocity of the leading vehicle and host vehicle (results from simulation).

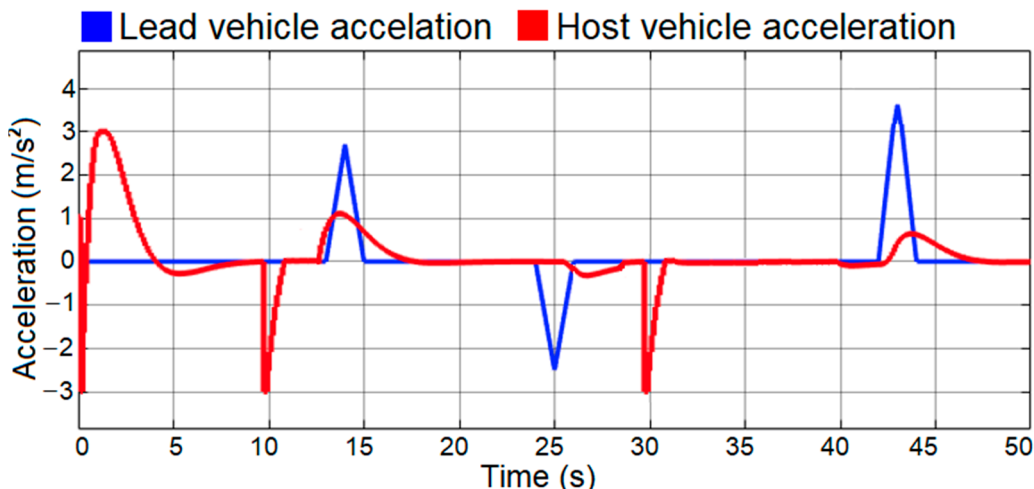


Figure 17. Acceleration of the leading vehicle and host vehicle (results from simulation).

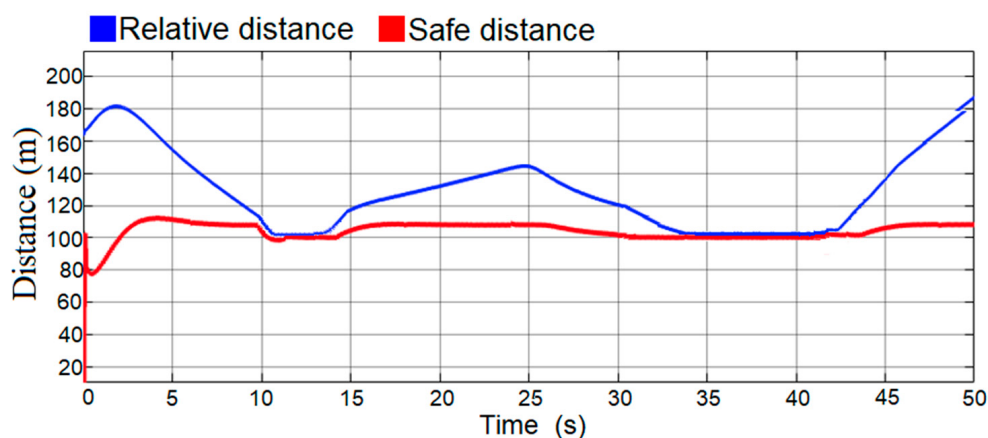


Figure 18. Relative distance and safe distance (results from simulation).

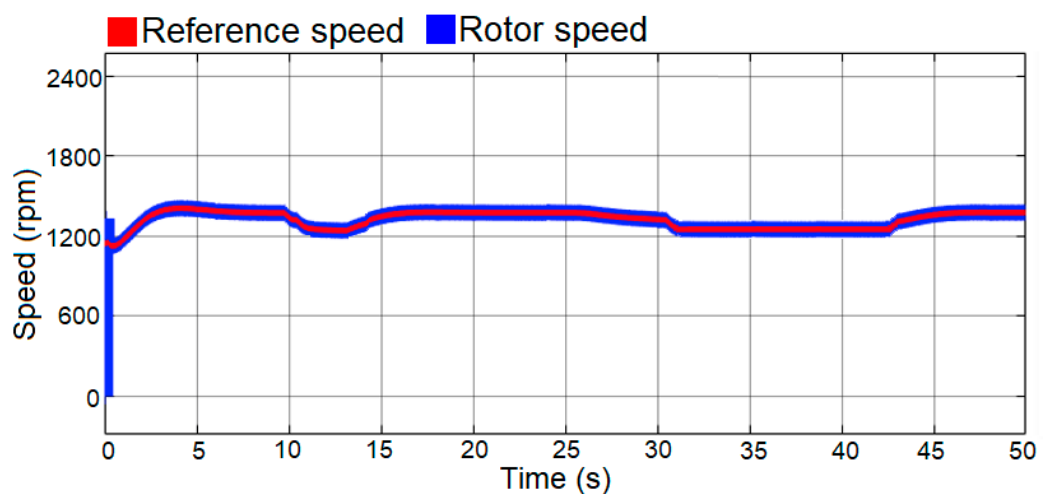


Figure 19. Reference speed and measured speed of the rotor (results from simulation).



Figure 20. Reference and load torque (results from simulation).

- Experimental results

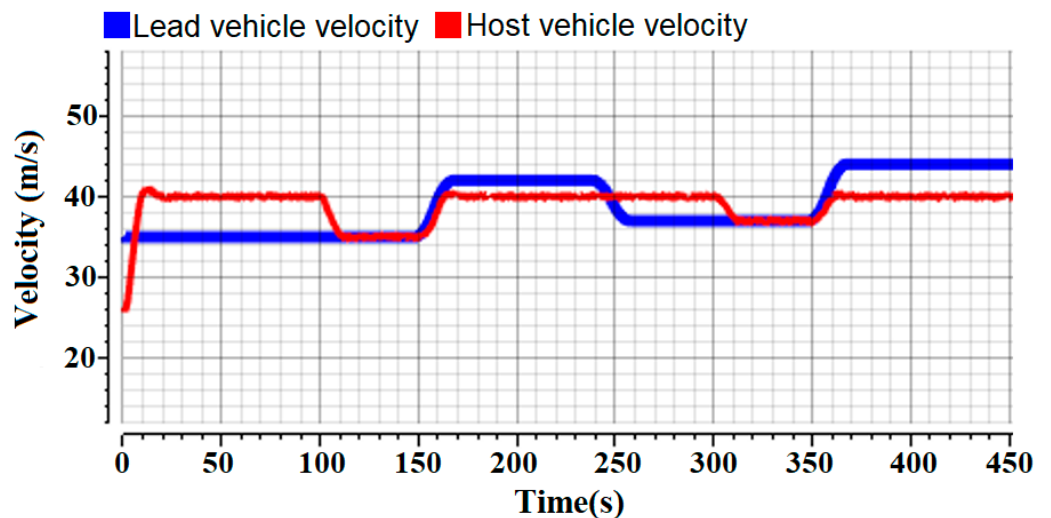


Figure 21. Velocity of the leading vehicle and host vehicle (experimental results).

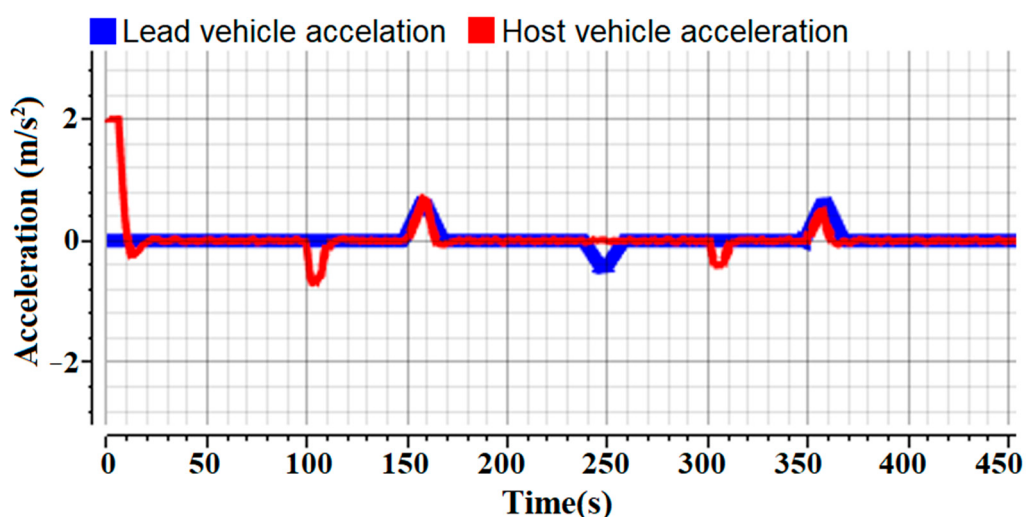


Figure 22. Acceleration of the leading vehicle and host vehicle (experimental results).

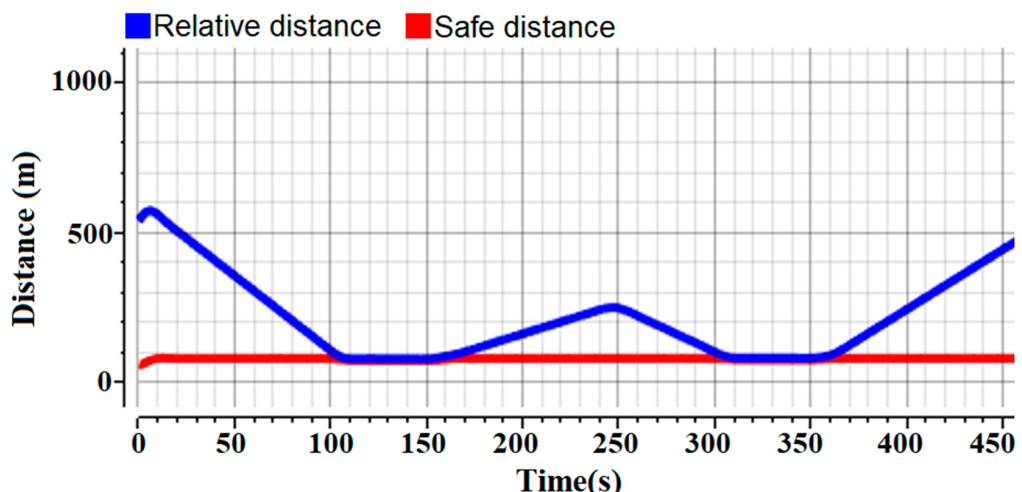


Figure 23. Relative distance and safe distance (experimental results).

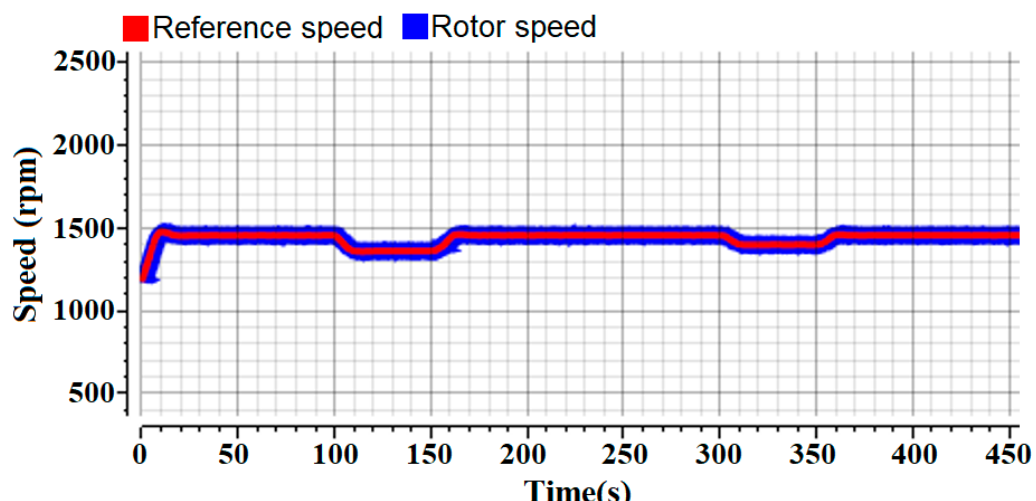


Figure 24. Reference and measured speed of the motor (experimental results).

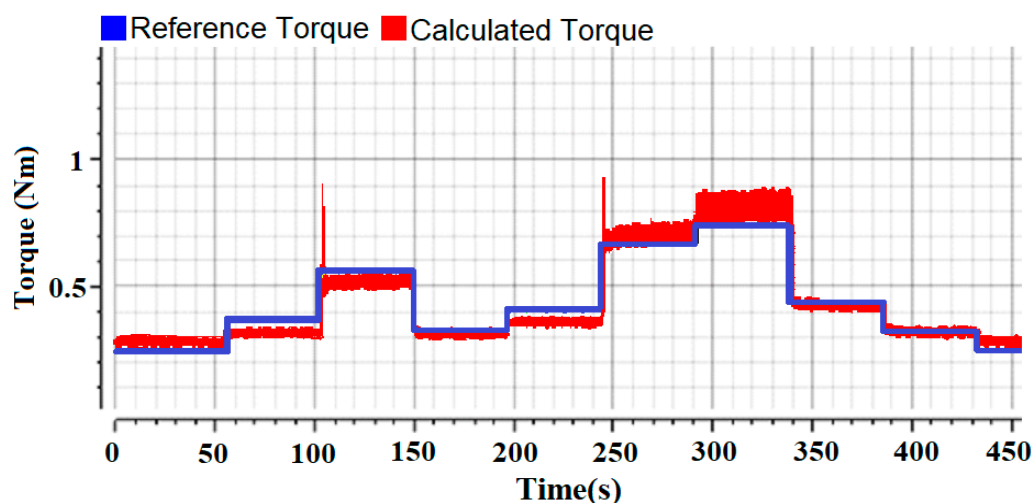


Figure 25. Reference and load torque (experimental results).

6. Discussion

In the results of the simulation and experimental setup, both results present the system response for an adaptive cruise control scenario. The tested scenario was as follows: based on the driver input and radar input, the adaptive cruise control system computed the corresponding acceleration/deceleration to ensure the set velocity and a safe distance. The acceleration/deceleration value was integrated to obtain the speed, which was added to the reference input of the field-oriented control. The ideal situation is when the vehicle is on a flat road with no leading vehicle in front, so the ACC block generates the corresponding acceleration to reach the set velocity and keep the velocity constant. A challenging scenario is when the vehicle is in a hill climbing situation; the load torque is bigger, the control loop must overcome the change, and there is a leading vehicle in front, so the velocity must be reduced to ensure a safe distance.

The tested scenario put the host vehicle in the situation of a leading vehicle in front, and the torque load changed, as in the case of hill climbing. The host car was driving at 40 m/s when the relative distance was larger than the safe distance. Every time the relative distance decreased, so the two vehicles approached each other, the ACC block generated a deceleration value so the velocity of the host vehicle was reduced to ensure a safe distance. The host vehicle velocity was kept constant at a value equal to the leading vehicle velocity; for the presented scenario, the host vehicle was running at 35 m/s or 36 m/s while the relative distance equaled the safe distance. When the leading vehicle was driving with a higher velocity, and the relative distance was larger than the safe distance, the ACC block generated an acceleration value and the host vehicle velocity was increased at the set value of 40 m/s. Figures 16 and 21 present the velocity responses of the two vehicles in the simulation and in the experimental setup. Figures 17 and 22 illustrate the corresponding acceleration/deceleration. The acceleration/deceleration of the host vehicle was computed by the ACC block, based on the set velocity, relative distance, and safe distance, presented in Figures 18 and 23.

The velocity variations were conducted in the presence of torque load, and the field-oriented control ensured the efficient control of the motor. As can be seen from the motor speed response from Figures 19 and 24, the rotor speed accordingly followed the reference speed, and, also, the torque response, as shown in Figures 20 and 25.

In the case of electric vehicle, the functionality of adaptive cruise control was easier because the acceleration/deceleration command was sent directly to the motor control block, without further components, no throttle, or throttle control. Additionally, the electric motor allowed both acceleration and deceleration by increasing and decreasing the reference value of the field-oriented control block. This paper does not present the mechanical braking system; only the brake provided by the motor is considered. In this

paper is presented only the electric parts of an EV, and it proves how a field-oriented control block and an adaptive cruise control can work together in the case of an electric vehicle.

7. Conclusions

This paper presents the concept of an adaptive cruise control system in the case of an electric vehicle, with an indirect field-oriented control using an induction machine. The system proposed was modeled and simulated in a MATLAB Simulink environment; then, a low-scale laboratory system was implemented, using a dSPACE platform. The adaptive cruise control scenario test was performed in the simulated system and, also, in the experimental setup, considering an electric vehicle system. If the driver set a constant driving speed using adaptive cruise control, the induction machine was controlled with field-oriented control to keep the vehicle running at the desired speed, regardless of the torque load of the motor. Additionally, when a leading car was detected in front of the host vehicle, the adaptive cruise control block generated a negative acceleration to reduce the velocity, and a safe distance was kept between the vehicles.

The following are proved by this study:

- The interaction between an adaptive cruise control system and indirect field-oriented control of the electric motor is presented, as well as how a good relationship between the two control strategies can improve the efficiency of electric vehicles.
- In the case of an adaptive cruise control scenario, a field-oriented control system for an induction machine proved good performance.
- A dSPACE platform was successfully used to develop a digital field-oriented control and a prototype electric traction system.
- The results obtained from the simulated system and from the experimental system prove the correct operation of the proposed implemented system.

Future work on this topic will be the implementation of an adaptive cruise control system based on artificial intelligence. The capabilities of artificial intelligence systems and special sensors in an advanced adaptive cruise control system can be implemented with many features to make driving easier, safer, and more economical.

Finally, this paper illustrates the operation of an adaptive cruise control in relation with an induction machine controlled in an indirect field-oriented manner considering an electric vehicle system concept.

Author Contributions: Conceptualization, D.M.P. and A.-M.P.; software, A.-M.P.; validation, A.-M.P. and D.M.P.; investigation, A.-M.P.; resources, A.-M.P. and D.M.P.; writing—original draft preparation, A.-M.P.; writing—review and editing, A.-M.P.; supervision, D.M.P. All authors have read and agreed to the published version of the manuscript.

Funding: This research received no external funding.

Institutional Review Board Statement: Not applicable.

Informed Consent Statement: Not applicable.

Data Availability Statement: Not applicable.

Acknowledgments: This paper was supported by the project “Entrepreneurial competences and excellence research in doctoral and postdoctoral programs-ANTREDOC”, a project co-funded by the European Social Fund.

Conflicts of Interest: The authors declare no conflict of interest.

References

1. Cars Guide: Reviews, News, and Advice. Available online: <https://www.carsguide.com.au/car-advice/how-many-cars-are-there-in-the-world-70629> (accessed on 25 March 2022).
2. Abo-Khalil, A.G.; Abdelkareem, M.A.; Sayed, E.T.; Maghrabie, H.M.; Radwan, A.; Rezk, H.; Olabi, A.G. Electric vehicle impact on energy industry, policy, technical barriers, and power systems. *Int. J. Thermofluids* **2022**, *13*, 100134. [CrossRef]

3. Poornesh, K.; Nivya, K.P.; Sireesha, K. A Comparative study on Electric Vehicle and Internal Combustion Engine Vehicles. In Proceedings of the International Conference on Smart Electronics and Communication (ICOSEC), Trichy, India, 10–12 September 2020. [CrossRef]
4. Aruna, P.; Vasan, P.V. Review on Energy Management System of Electric Vehicles. In Proceedings of the 2019 2nd International Conference on Power and Embedded Drive Control (ICPEDC), Chennai, India, 1–23 August 2019; pp. 371–374. [CrossRef]
5. Madhusudhanan, A.K. A method to improve an electric vehicle’s range: Efficient Cruise Control. *Eur. J. Control.* **2019**, *48*, 83–96. [CrossRef]
6. Diba, F.; Arora, A.; Esmailzadeh, E. Optimized robust cruise control system for an electric vehicle. *Syst. Sci. Control. Eng. Open Access J.* **2014**, *2*, 175–182. [CrossRef]
7. Chu, H.; Dong, S.; Hong, J.; Chen, H.; Gao, B. Predictive Cruise Control of Full Electric Vehicles: A Comparison of Different Solution Methods. *IFAC-PapersOnLine* **2021**, *54*, 120–125. [CrossRef]
8. Kara, M.Y.; Gol, E.A. Adaptive Cruise Control with Timed Automata. *IFAC-PapersOnLine* **2020**, *53*, 1918–1923. [CrossRef]
9. Dong, S.; Gao, B.; Liu, Q.; Liu, J.; Chen, H. A Computationally Efficient Predictive Cruise Control for Automated Electric Vehicles. *IFAC-PapersOnLine* **2020**, *53*, 14173–14178. [CrossRef]
10. Shaout, A.; Jarrah, M.A. Cruise control technology review. *Comput. Electr. Eng.* **1997**, *23*, 259–271. [CrossRef]
11. Brugnolli, M.M.; Angélico, B.A.; Laganá, A.A.M. Predictive Adaptive Cruise Control Using a Customized ECU. *IEEE Access* **2019**, *7*, 55305–55317. [CrossRef]
12. Smithsonian Magazine. Available online: <https://www.smithsonianmag.com/innovation/sightless-visionary-who-invented-cruise-control-180968418/> (accessed on 25 March 2022).
13. Hidayatullah, M.R.; Juang, J.-C. Adaptive Cruise Control with Gain Scheduling Technique under Varying Vehicle Mass. *IEEE Access* **2021**, *9*, 144241–144256. [CrossRef]
14. Wang, C.; Jaidaa, A.; Wang, Z.; Lu, L. An Effective Decoupling Control with Simple Structure for Induction Motor Drive System Considering Digital Delay. *Electronics* **2021**, *10*, 3048. [CrossRef]
15. Arpit, G.; Singh, H.P.; Pandey, K. Advance speed control of three phase induction motor using field-oriented control method. *Mater. Today Proc.* **2021**. [CrossRef]
16. Kostal, T.; Koblre, P. Induction Machine On-Line Parameter Identification for Resource-Constrained Microcontrollers Based on Steady-State Voltage Model. *Electronics* **2021**, *10*, 1981. [CrossRef]
17. Hegazy, O.; Barrero, R.; van Mierlo, J.; Lataire, P.; Omar, N.; Coosemans, T. An Advanced Power Electronics Interface for Electric Vehicles Applications. *IEEE Trans. Power Electron.* **2013**, *28*, 5508–5521. [CrossRef]
18. Petri, A.; Petreus, D. Vector Control of Induction Machine Used in Electric Vehicle. In Proceedings of the 2020 43rd International Spring Seminar on Electronics Technology (ISSE), Demanovská Valley, Slovakia, 14–15 May 2020; pp. 1–5. [CrossRef]
19. AAliasand, E.; Josh, F.T. Selection of Motor for an Electric Vehicle: A Review. *Mater. Today Proc.* **2020**, *24*, 1804–1815. [CrossRef]
20. Quintero-Manríquez, E.; Sanchez, E.N.; Antonio-Toledo, M.E.; Muñoz, F. Neural control of an induction motor with regenerative braking as electric vehicle architecture. *Eng. Appl. Artif. Intell.* **2021**, *104*, 104275. [CrossRef]
21. Reshma, S.; Samuel, E.R.; Unnikrishnan, A. A Review of various Internal Combustion Engine and Electric Propulsion in Hybrid Electric Vehicles. In Proceedings of the 2019 2nd International Conference on Intelligent Computing, Instrumentation and Control Technologies, Kannur, India, 5–6 July 2019. [CrossRef]
22. Bimal, K.B. *Modern Power Electronics and AC Drivers*; Prentice Hall PTR: Upper Saddle River, NJ, USA, 2002; pp. 29–96, 333–435.
23. Bhuvaneswari. Vector Controlled Induction Machine Applied to Automobile System. *Electr. Power Compon. Syst.* **2003**, *31*, 47–60. [CrossRef]
24. Nisha, G.K.; Lakaparampil, Z.V.; Ushakumari, S. Torque capability improvement of sensorless FOC induction machine in field weakening for propulsion purposes. *J. Electr. Syst. Inf. Technol.* **2017**, *4*, 173–184. [CrossRef]
25. Bahloul, M.; Chrifi-Alaoui, L.; Drid, S.; Souissi, M.; Chaabane, M. Robust sensorless vector control of an induction machine using Multiobjective Adaptive Fuzzy Luenberger Observer. *ISA Trans.* **2018**, *74*, 144–154. [CrossRef]
26. Azzoug, Y.; Sahraoui, M.; Pusca, R.; Ameid, T.; Romary, R.; Antonio, J.; Cardoso, M. High-performance vector control without AC phase current sensors for induction motor drives: Simulation and real-time implementation. *ISA Trans.* **2021**, *109*, 295–306. [CrossRef]
27. Kiselev, A.; Kuznetsov, A. Motor drive control of a full-electric vehicle using generalized predictive control algorithm. In Proceedings of the 2014 IEEE International Electric Vehicle Conference (IEVC), Florence, Italy, 17–19 December 2014; pp. 1–5. [CrossRef]
28. Su, J.; Gao, R.; Husain, I. Model Predictive Control Based Field-Weakening Strategy for Traction EV Used Induction Motor. *IEEE Trans. Ind. Appl.* **2018**, *54*, 2295–2305. [CrossRef]
29. Gashtil, H.; Pickert, V.; Atkinson, D.J.; Dahidah, M.; Giaouris, D. Improved Voltage Boundary with Model-Based Control Algorithm for Increased Torque in the Field Weakening Region of Induction Machines. *IEEE Trans. Transp. Electrif.* **2021**, *7*, 1600–1614. [CrossRef]
30. Pananurak, W.; Thanok, S.; Parnichkun, M. Adaptive cruise control for an intelligent vehicle. In Proceedings of the 2008 IEEE International Conference on Robotics and Biomimetics, Bangkok, Thailand, 8 May 2009. [CrossRef]
31. Chu, H.; Guo, L.; Yan, Y.; Gao, B.; Chen, H. Self-Learning Optimal Cruise Control Based on Individual Car-Following Style. *IEEE Trans. Intell. Transp. Syst.* **2020**, *22*, 6622–6633. [CrossRef]